Carcinogenesis vol.29 no.6 pp.1290–1297, 2008
doi:10.1093/carcin/bgn094
Advance Access publication April 15, 2008

Lack of DNA mismatch repair protein MSH6 in the rat results in hereditary non-polyposis colorectal cancer-like tumorigenesis

Ruben van Boxtel[1], Pim W.Toonen[1], Henk S.van Roekel[1], Mark Verheul[1], Bart M.G.Smits[1,3], Jeroen Korving[1], Alain de Bruin[2] and Edwin Cuppen[1,*]

[1]Hubrecht Institute for Developmental Biology and Stem Cell Research, Cancer Genomics Center, Uppsalalaan 8, 3584 CT Utrecht, The Netherlands and [2]Department of Pathobiology, Faculty of Veterinary Medicine, Utrecht University, Yalelaan 1, 3584 CL Utrecht, The Netherlands

[3]Present address: Department of Oncology, McArdle Laboratory for Cancer Research, University of Wisconsin-Madison, 1400 University Avenue, Madison, WI 53706, USA

[*]To whom correspondence should be addressed. Tel: +31 30 2121969; Fax: +31 30 2516554;
Email: e.cuppen@niob.knaw.nl

To understand genetic instability in relation to tumorigenesis, experimental animal models have proven very useful. The DNA mismatch repair (MMR) machinery safeguards genomic integrity by repairing mismatches, insertion or deletion loops and responding to genotoxic agents. Here, we describe the functional characterization of a novel rat mutant model in which the MMR gene *Msh6* has been genetically inactivated by *N*-ethyl-*N*-nitrosourea-driven target-selected mutagenesis. This model shows a robust mutator phenotype that is reflected by microsatellite instability and an increased germ line point mutation frequency. Consequently, these rats develop a spectrum of tumors with a high similarity to atypical hereditary non-polyposis colorectal cancer in humans. The MSH6 knockout rat complements existing models for studying genetic instable tumorigenesis as it provides experimental opportunities that are not available or suboptimal in current models.

Introduction

The mismatch repair (MMR) system recognizes mismatches that are introduced during DNA replication and surpass the proofreading activity of DNA polymerase. The MMR machinery has been highly conserved in evolution, and the prototypic system was first elucidated in *Escherichia coli* (1). In this model, a mismatch is recognized by the MutS homodimer followed by binding of the MutL homodimer and activation of the repair pathway. This induces the excision and resynthesis of the error-containing DNA strand. In eukaryotes, MutS function is separated in the recognition of single-base mismatches and small insertion or deletion loops of one or two extra helical nucleotides by MutSα and the recognition of larger insertion or deletion loops by MutSβ. Both are heterodimers consisting of MSH2–MSH6 and MSH2–MSH3, respectively (2).

Besides maintaining the genomic integrity during replication, the MMR system has been shown to mediate DNA damage-induced apoptosis. Cell lines deficient for MMR are more resistant to cell death induced by alkylating agents (3,4), antimetabolites and intrastrand cross-linking agents (5). Two hypotheses have been proposed to explain MMR-mediated apoptosis. The repeated activation of MMR due to wrong nucleotide insertion by polymerase at the site of DNA damage may cause double-stranded breaks, which ultimately results in lethality (6). Alternatively, the MMR system may function as a molecular sensor that can directly activate the apoptotic machinery in case of high levels of DNA damage (7).

In humans, mutations in MMR genes have been linked to hereditary non-polyposis colorectal cancer (HNPCC), also referred to as Lynch syndrome, which is characterized by early-onset colon cancer (8). Mutations in the *Msh6* gene have been associated with an atypical HNPCC phenotype characterized by a late onset and a high occurrence of extracolonic tumors, especially in the endometrium (9). A hallmark of MMR deficiency in HNPCC tumors is a significantly higher mutation rate, like the instability of simple repeat lengths during DNA replication (10). This phenomenon is referred to as microsatellite instability (MSI) and has proven to be a powerful tool to diagnose HNPCC tumors (11).

Mouse knockout models have provided insight about *in vivo* deficiency of MMR function. Complete loss of MMR recognition in the *msh2*$^{-/-}$ mouse results in a strong reduction in the survival of these mice with a median survival time of 5–6 months (12). At an early stage in life, these mice develop lymphomas followed by a later onset of adenocarcinomas in the gastrointestinal tract (12,13). Inactivation of the *Msh6* gene in mice also results in a decreased life span; however, this survival seems to be prolonged compared with *msh2*$^{-/-}$ mice. *Msh6*$^{-/-}$ mice show a median survival time of 6–10 months and predominantly develop lymphomas and rarely intestinal tumors (14,15). Deletion of the *Msh3* gene in mice did not induce a cancer phenotype; however, deletion of this gene in a MSH6-deficient background led to a cancer phenotype indistinguishable from that of the *msh2*$^{-/-}$ mouse, suggesting redundancy between MSH6 and MSH3 (14). Although mouse knockout models have provided very valuable insight in mammalian MMR, modeling human HNPCC has only been successful in a limited way. First, heterozygous MMR mouse knockouts do not develop tumors and second, the spectra of tumors that develop in homozygous knockouts differ from the human situation. The human HNPCC phenotype primarily shows colorectal tumors, whereas the mouse models develop primarily lymphomas and tumors in the small intestine (12,15). Furthermore, the high occurrence of endometrial cancers found in human atypical HNPCC, especially in the case of *Msh6* germ line mutations (9), is not reflected by the mouse model. Hence, novel models have the potential to complement exiting model systems.

Over the last decades, the rat has become an important genetic model system (16,17). The complete genome sequence of the rat is now available (18) and recently developed techniques make it possible to generate genetic knockouts using a target-selected *N*-ethyl-*N*-nitrosourea (ENU)-driven mutagenesis approach (19,20). There are indications that some human cancer syndromes, which have been difficult to model in genetically engineered mice, are more closely reflected in rats. One example is the recent report of the Pirc rat that carries a knockout allele of the *Apc* gene. The mouse knockout model, Apc^{min}, which has been studied for decades, develops primarily tumors in the small intestine (21), whereas the rat knockout primarily develops colonic tumors (22), similar to human patients (23). Another example is the inability to study the loss-of-function of BRCA1 or BRCA2, which are often mutated in human breast tumors (24), because knocking out these genes in mice negatively affected viability. It turned out to be possible to generate viable *Brca2* knockout rats that develop tumors, although no increased incidence for breast tumor development was observed (20,25). Nevertheless, this rat provides a unique model to study the *in vivo* role of this gene in tumorigenesis.

Here, we describe the genetic inactivation of the *Msh6* gene in the rat and the phenotypic consequences. A premature stop codon in the *Msh6* gene, introduced using an ENU-driven target-selected mutagenesis approach (19), was shown to result in a full functional knockout of the gene. Primary characterization of this *msh6*$^{-/-}$ rat revealed a strong mutator phenotype resulting in a reduced life span due to the development of different types of tumors, including lymphomas and endometrial cancers.

Abbreviations: ENU, *N*-ethyl-*N*-nitrosourea; HNPCC, hereditary non-polyposis colorectal cancer; MMR, mismatch repair; MSI, microsatellite instability; PCR, polymerase chain reaction.

Materials and methods

Animals

All experiments were approved by the Animal Care Committee of the Royal Dutch Academy of Science according to the Dutch legal ethical guidelines. Experiments were designed to minimize the number of required animals and their suffering. The MSH6 knockout rat (Msh6^{1Hubr}) was generated by target-selected ENU-driven mutagenesis [for detailed description, see (19)]. Briefly, high-throughput resequencing of genomic target sequences in progeny from mutagenized rats revealed an ENU-induced premature stop codon in exon 4 of the *Msh6* gene in a rat (Wistar/Crl background). The heterozygous-mutant animal was outcrossed at least three times to eliminate confounding effects from background mutations induced by ENU. To obtain homozygous animals, the heterozygous offspring were crossed in. At 3 weeks of age, ear cuts were taken and used for genotyping. Genotypes were reconfirmed after experimental procedures were completed. Animals were housed under standard conditions in groups of two to three per cage per gender under controlled experimental conditions (12 h light–dark cycle, 21 ± 1°C, 60% relative humidity and food and water *ad libitum*).

Genotyping

Genotyping was performed using the KASPar SNP Genotyping System (KBiosciences, Hoddesdon, UK) and gene-specific primers (forward common, CAGTGGACCCACTATCTGGTA; reverse a1, GAAGGTGACCAAGTTCATGCTCTTCTCTGGCTTAAGCCATTCTA; reverse a2, GAAGGTCGGAGTCAACGGATTCTCTTCTCTGGCTTAAGCCATTCTT). Briefly, a polymerase chain reaction (PCR) was carried out using the optimal thermocycling conditions for KTaq (94°C for 15 min; 20 cycles of 94°C for 10 s, 57°C for 5 s and 72°C for 10 s; followed by 18 cycles of 94°C for 10 s, 57°C for 20 s and 72°C for 40 s; GeneAmp9700, Applied Biosystems, Foster City, CA). The PCR reaction contained 2 µl DNA solution, 1 µl 4× reaction mix, 165 nM reverse primer a1 and a2, 412.5 nM of the common forward primer, 0.025 µl KTaq polymerase and 0.4 mM $MgCl_2$ in a total volume of 4 µl. Samples were analyzed in a PHERAstar plate reader (BMG Labtech, Offenburg, Germany) and data were analyzed using Klustercaller software (KBiosciences). All genotypes were confirmed in an independent reaction.

Western blot analysis

Proteins were extracted by adding lysis buffer (1% sodium dodecyl sulfate, 1.0 mM sodium orthovanadate and 10 mM Tris, pH 7.4) to ∼0.25 g of tissue or cultured cells. The protein was separated on a sodium dodecyl sulfate gel (6% acrylamide gradient, Bio-Rad, Hercules, CA) and transferred to a nitrocellulose membrane. The membrane was incubated overnight at 4°C with a 1:100 dilution of a monoclonal mouse anti-human MSH6 antibody (BD Biosciences Pharmingen, Franklin Lakes, NJ) in blocking buffer followed by an incubation for 2 h with peroxidase-conjugated anti-mouse IgG diluted 1:2500 in blocking buffer at room temperature. Protein bands were detected by using the enhanced chemiluminescence detection method (Amersham Biosciences, Buckinghamshire, UK). Cell lysate from human embryonic kidney cells was used as a control and total protein was measured by Coomassie brilliant blue staining.

MSI analysis

A simple repeat containing a repetitive stretch of $(CA)_{40}$ (chr14:85120966-85121141, RGSC 3.4) was PCR amplified using the following primers: 5′-6FAM^{TM}-TTCAACCACAATCTCGACAG-3′ (forward) and 5′-AGGCATGAGTTCTGAGGTTC-3′ (reverse); the simple repeat (contig) with the stretch of $(CA)_{36}$ (chr13:105939209-105939433) was PCR amplified using the following primers: 5′-6FAM^{TM}-TGGCACAGGTGTTTAGTGTC-3′ (forward) and 5′-TGCAGAAGAAATGAGAGGTG-3′ (reverse); for PCR amplifying, the simple repeat containing a $(G)_{20}$ (chr3:105633672-105633851) 5′-VIC®-CATTCTGGAAGTGACTGCTG-3′ (forward) and 5′-TCCACGATACTGCAATTCTC-3′ (reverse) were used and the simple repeat containing the stretch of $(A)_{30}$ (chr8:118654926-118655555) was PCR amplified using the following primers: 5′-NED^{TM}-GCCCTCTTCTGGTGTATCTG-3′ (forward) and 5′-AGCTTCATCCGTTAGTGTGG-3′ (reverse). The appropriate volume of PCR product was mixed with 0.5 µl of GeneScan^{TM}–500 LIZ^{TM} size standard (Applied Biosystems) in 5 µl of milli-Q-grade water, denaturated for 5

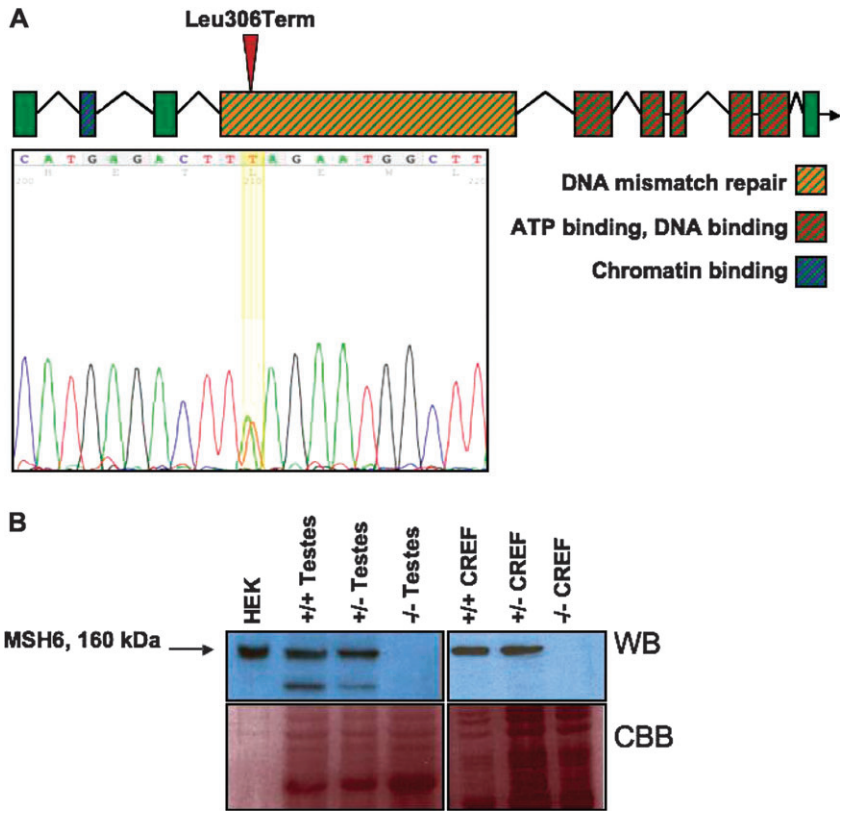

Fig. 1. Molecular characterization of the *msh6*$^{-/-}$ rat. (**A**) Genomic organization of the *Msh6* gene in the rat genome. The arrow marks the position of the ENU-induced mutation that results in a premature stop codon. The sequence trace indicates the T to A transition in a heterozygous rat. (**B**) Western blot (WB) of testes and cultured rat embryonic fibroblast (CREF) lysates stained with antibodies against human MSH6 (160 kDa). Lysate of human embryonic kidney (HEK) cells was loaded as a positive control. MSH6 protein is completely absent in *msh6*$^{-/-}$ testes and cultured rat embryonic fibroblast. Coomassie brilliant blue staining (CBB) was used as a control for protein loading.

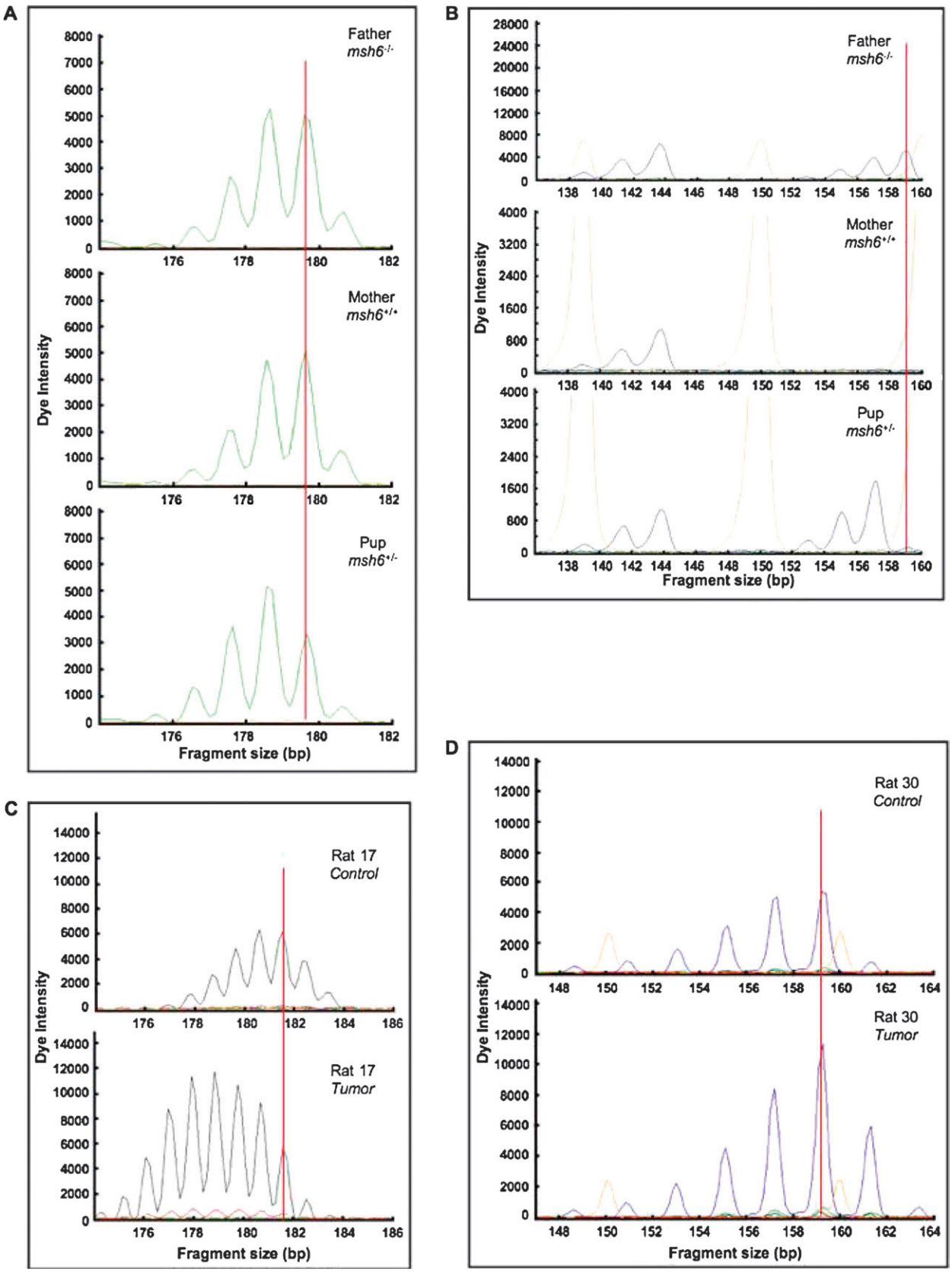

Fig. 2. MSI in the germ line and tumors. (**A**) A mononucleotide repeat of 20 repetitive subunits $(G)_{20}$ was analyzed in a cross between an *msh6*$^{-/-}$ father and a wild-type mother and their *msh6*$^{+/-}$ offspring. The DNA of the parents and pups was isolated from ear and tail cuts, respectively. The red line indicates the size of the most prominent amplification product in both parents. In the DNA sample of the offspring, one of the alleles has lost one repetitive subunit. (**B**) Fragment analysis of a dinucleotide repeat $(CA)_{36}$ that is polymorphic between the founder animals. As a result, progeny is heterozygous for this marker and the depicted F1 animal shows a deletion of one repetitive subunit in the larger allele, which was inherited from the *msh6*$^{-/-}$ father. (**C**) Mononucleotide repeat instability in tumors.

min at 95°C and subsequently run on an AB3730WL capillary DNA analyzer (Applied Biosystems). Product lengths were analyzed using Genemapper software (Applied Biosystems).

Point mutation analysis

Seven hundred and sixty-eight preselected amplicons were amplified using a nested PCR setup followed by dideoxy sequencing. Sequencing products were purified by ethanol precipitation in the presence of 40 mM sodium acetate and analyzed on a 96-capillary 3730XL DNA analyzer (Applied Biosystems), using the standard RapidSeq protocol on 36 cm array. Sequences were analyzed for the presence of heterozygous mutations using PolyPhred (26) and in-house developed software. All candidate mutations were verified in independent PCR and sequencing reactions.

Analysis of tumors

Animals were scarified by CO_2/O_2 suffocation. Tumors, when found, and organs including the gastrointestinal tract, lungs, liver, kidneys, spleen and thymus were removed and fixed in phosphate-buffered 4% formaldehyde. Representative tissues from the tumors and organs were processed and embedded in paraffin. All tissues were prepared for hematoxylin and eosin stain. Lymphomas were studied for immunotyping. After deparaffination, the sections were heated with citrate buffer, pH 6.0, for antigen retrieval. The endogenous peroxidase activity was blocked with 1% H_2O_2 in methanol for 30 min. The slides were incubated with 10% normal serum for 10 min followed by an incubation with mouse anti-CD79 (1:80, M7051, DAKO, Glostrup, Denmark) or rabbit anti-CD3 (1:1500, CMC 365, Cell Marque Corp., Rocklin, CA) overnight at 4°C. After 30 min incubation with horse anti-mouse/biotin (1:125, BA-2000, Vector, Peterborough, UK) or goat anti-rabbit/biotin (1:250, E0432, DAKO), the slides were incubated with avidin–biotin peroxidase complex (PK-4000, Vector) for 30 min. Visualization was performed with 3,3-diaminobenzidine solution (Sigma, Zwijndrecht, NL) for 10 min. Nuclei were stained with Mayer's hematoxylin. After dehydrazition, the slides were mounted with Eukitt (O. Kindler GmbH & Co., Freiburg, Germany). Washing steps were preformed with phosphate-buffered saline–Tween, antibody dilutions and avidin-biotin peroxidase complex were made with phosphate-buffered saline.

For MSI analysis, slides were deparaffinated and lysed overnight followed by phenol–chloroform (1:1, vol:vol) extraction. DNA was precipitated by adding 300 µl isopropanol and mixing and centrifuging for 20 min at 21 000*g* at 4°C. The supernatant was discarded and pellets were washed with 70% ethanol and dissolved in 50 µl 10 mM Tris–HCL (pH 8.0).

Results

Generation of the MSH6 knockout rats

In a large ENU-driven target-selected mutagenesis screen, we identified a rat carrying a heterozygous mutation in the *Msh6* gene (19). This T to A transition in exon 4 resulted in a premature stop codon at position 306 (Figure 1A). After outcrossing the mutant rat, heterozygous offspring was used to obtain homozygous-mutant rats, which occurred in a Mendelian fashion (data not shown). The homozygous mutants showed normal growth and fertility. Confirmation of the *Msh6* gene knockout phenotype at the molecular level was established by western blotting, showing that the full-length MSH6 protein of ~160 kDa in the testes of $msh6^{+/+}$ and $msh6^{+/-}$ males was completely lacking in the testes of $msh6^{-/-}$ males (Figure 1B). We could not detect any truncated protein, suggesting that either the messenger RNA with the premature stop codon or the truncated protein is unstable, due to non-sense-mediated decay or protein folding defects, respectively. Cell lysates of cultured rat embryonic fibroblasts also showed complete absence of MSH6 in homozygous-mutant cultures, further confirming these results.

MSH6 knockout rats show a germ line mutator phenotype

To confirm loss of MSH6 function, we analyzed the presence of MSI in the germ line of $msh6^{-/-}$ males. Two mononucleotide repeats, $(G)_{20}$ and $(A)_{30}$, and two dinucleotide repeats, $(CA)_{36}$ and $(CA)_{40}$, were analyzed in the outcrossed offspring of 9 $msh6^{-/-}$ males and 19 $msh6^{+/+}$ males. In both mononucleotide repeats (Figure 2A) and dinucleotide repeats (Figure 2B), MSI was observed as a monoallelic change of the length of the tested repeat. Although for some of the repeats the paternal (−/−) and maternal (+/+) contribution could not be distinguished (Figure 2A), in other cases the size of the repeat was polymorphic within the strain and showed that the MSI phenotype is exclusively contributed by the paternal allele on an $msh6^{-/-}$ background (Figure 2B). In total, 168 progeny from 9 homozygous-mutant males were tested and revealed that germ line MSI occurred in all males and in all the repeats tested (Table I). None of the 100 offspring samples from 19 control wild-type males and females showed MSI.

Because the MSH6 protein is also involved in the recognition of single-base mismatches introduced during DNA replication, we anticipated finding an elevated spontaneous germ line mutation frequency. Indeed, whereas the mammalian germ line mutation frequency is estimated $\sim 1 \times 10^{-8}$ per bp per generation (27), high-throughput resequencing of preselected amplicons, followed by heterozygous mutation discovery in DNA samples from the offspring of two $msh6^{-/-}$ males and wild-type females, revealed three mutations in 8.3×10^6 resequenced base pairs (twice a C > T and once a G > A transition; supplementary Table I is available at *Carcinogenesis* Online). This indicates an ~30-fold increased spontaneous single-base pair mutation rate of $\sim 3.6 \times 10^{-7}$ per bp in the male germ line of the $msh6^{-/-}$ rat. As a control, the same amplicons were sequenced in DNA samples from the offspring of four wild-type males and no mutation was found in the 6.6×10^6 bp, indicating that the wild-type mutation rate in the genetic background used is $< 1.5 \times 10^{-7}$ per bp.

MSH6 knockout rats show a reduced life span and develop tumors

Studies in the mouse have shown that MSH6 deficiency results in a reduced life span due to the development of different types of tumors (14,15). Homozygous-mutant rats showed a median survival time of 14 months, whereas 95% of wild-type rats normally survive at this age (supplementary Figure 1 is available at *Carcinogenesis* Online). After 18 months, all the $msh6^{-/-}$ rats had become moribund, showing a tumor incidence of ~88%. These results are consistent with the observation that MSH6-deficient mice show a reduced life span although they exhibited a median survival time of only 6–10 months (14,15).

Each rat was subjected to a complete necropsy and histopathological analysis. The first tumors were detected at 9 months of age in different locations and the first affected rats were males. Representative histological specimens of the tumor spectra that were observed are shown in Figure 3 and the complete data are summarized in Table II. Macroscopical examination revealed a significantly enlarged spleen, which was the result of infiltration of lymphomas. In total, 8 of 17 rats developed highly invasive lymphomas in the spleen, liver, kidney, lung and mediastinum (Figure 3). Histological analysis of the lymphomas revealed that neoplastic lymphocytes were organized in sheets separated by fine fibrovascular stroma. The round cells were uniform and of medium size with scant cytoplasm and round to ovoid nuclei containing fine chromatin and occasionally a prominent nucleolus located centrally (lymphoblastic lymphoma). Sheets of neoplastic cells infiltrate into the surrounding tissue and occasionally into vascular structures. Multiple areas within the neoplasm show apoptosis characterized by pyknotic and fragmented nuclei and bright eosinophilic cytoplasm (starry sky pattern). To ascertain the cellular origin of the lymphomas, sections of tumors were stained with CD79, a B-cell-specific antibody and a CD3 antibody that is T cell specific. Of these, seven were determined to be B-cell lymphoblastic lymphoma and one was a T-cell lymphoblastic lymphoma.

Other tumors found in male $msh6^{-/-}$ rats included a testicular Leydig cell tumor and a mammary fibroadenoma and adenocarcinoma. Four females suffered from vaginal bleeding and histological

Three repetitive subunits in a mononucleotide repeat of 30 repetitive subunits $(A)_{30}$ were deleted in the DNA of tumor tissue (mediastinum) as compared with control DNA (ear cut). (**D**) Dinucleotide repeat instability in the DNA of tumor tissue (mediastinum) compared with control DNA (liver). The orange peaks represent the size marker that was loaded to determine the size of the PCR product.

Table I. MSI in the germ line of MSH6-deficient rats

Father (genotype)[a]	$(CA)_{36}$	$(CA)_{40}$	$(G)_{20}$	$(A)_{30}$	Pups tested[b]
F (−/−)	1	3	2	0	17
G (−/−)	1	2	3	1	24
HA (−/−)	0	1	1	0	18
I (−/−)	0	1	2	0	9
J (−/−)	2	0	1	3	22
K (−/−)	0	2	1	0	14
L (−/−)	1	0	0	2	3
M (−/−)	0	2	1	0	14
N (−/−)	2	3	1	3	47
Average MSI % of total pups (±SEM)	6 (±4)	9 (±2)	8 (±2)	10 (±7)	Total pups tested = 168
Control (+/+) $n = 19$	0	0	0	0	Total pups tested = 100

[a]DNA was isolated from ear cuts.
[b]DNA was isolated from tail cuts.

evaluation revealed the presence of endometrial carcinomas (Figure 3D) in three animals and uterine leiomyosarcoma in one female (Figure 3C). One female developed a gastric squamous cell carcinoma (Figure 3F). Notably, some of the tumors reached large sizes, like some of the lymphomas that had an estimated diameter in excess of 3 cm. Remarkably, the leiomyosarcoma in the uterus reached a diameter of ~5 cm and also the gastric tumor reached a diameter of ~2 cm (Table II).

Tumors of msh6$^{-/-}$ rats show MSI

To confirm the presence of genetic instable tumorigenesis in the *msh6*$^{-/-}$ rat, we analyzed the tumors for MSI. The four simple repeats described above were PCR amplified using DNA that was isolated from tumor tissues or control tissues (ear cuts or liver samples) and the product lengths were compared. Ten of 15 tumors showed length polymorphisms in at least one of the four examined simple repeats (Table II). All 10 tumors displayed mononucleotide repeat instability (Figure 2C) and 3 showed also dinucleotide repeat instability (Figure 2D). Some microsatellites were found to be highly unstable in the tumors, illustrated by deletions of up to seven repetitive subunits and the presence of biallelic changes (supplementary Table II is available at *Carcinogenesis* Online). As expected, the longest mononucleotide microsatellite that was studied, $(A)_{30}$, was found to be the most instable repeat.

Discussion

Carcinogenesis is believed to result from the accumulation of genomic mutations that change cells characteristics, which eventually result in the ability to proliferate and form tumors. DNA can be damaged by cellular metabolites and environmental agents, like alkylating agents, which are widespread environmental mutagens that alter the chemical structure of DNA and cause G–T mismatches after subsequent replication (28). Such damage can be recognized by MMR and indeed two of the three spontaneous mutations found in the rat MSH6-deficient germ line are probably to be unrecognized C to T transitions. Furthermore, mutations are generated because DNA polymerases make mistakes, although the fidelity of DNA polymerases is extremely accurate (29). The initiation of tumorigenesis resulting from genomic mutations can be explained by the mutator phenotype hypothesis—mutations in genes that function in the maintenance of genomic stability, like MMR genes, increase the mutation rate leading to a cascade of gene inactivation (30). Alternatively, carcinogenesis has also been explained by increased selective advantages of cells as a result of mutagenesis (31). MutSα has been found to play a role in DNA damage-induced apoptosis (4) and inactivation would result in a selective advantage. In this model, the associated genetic instability would only be a secondary effect. Both hypotheses are not mutually exclusive and could explain the onset of tumor development in the MSH6 knockout rat. Deletion of the MMR system will result in both the accumulation of DNA damage like frameshifts and point mutations, causing a mutator phenotype, and a selective advantage. Indeed, large-scale mutation discovery in a large set of tumors revealed extremely elevated somatic mutation prevalence in MMR-deficient cancer types (32).

Using ENU-driven target-selected mutagenesis, we have generated a rat knockout model of the MutSα component MSH6 (19), which shows all the features of a mutator phenotype. First, instability of both mono- and dinucleotide repeats was observed in both the mutant germ line as in tumors, but not in the wild-type germ line, confirming the role of MSH6 in the recognition of small insertion or deletion loops. MSI can result in hypermutability of expressed genes due to out-of-frame mutations (33) and because repetitive sequences have also been found in the coding regions of the *Msh6* gene itself, it is thought to be responsible for loss of heterozygosity in humans by mutating the wild-type allele (34). In mice lacking MSH6, replication error phenotype was observed at mononucleotide repeats in small intestinal epithelial cells that carried a *lac*I mutational reporter (35), and instability of dinucleotide repeats was observed in tumors (15). The frequency of MSI in the tumors of the *msh6*$^{-/-}$ rat that was found in this study is much higher as compared with that found in the mouse (36), which could be due to differences in the length of the simple repeats that were tested. Most tumors displayed MSI at $(A)_{30}$ (10 of 15 tumors), but for a much smaller repeat $(G)_{20}$ MSI frequency is much lower (2 of 15 tumors). Testing longer simple repeats increases the sensitivity of the analysis without generating false positives, which is illustrated by the absence of length polymorphisms in the wild-type germ line.

Second, accumulation of point mutations as a result of MMR deficiency can also attribute to the mutator phenotype. Indeed, lack of MSH6 results in a higher spontaneous germ line mutation rate compared with the wild-type germ line. Although the test groups were relatively small, the chance of discovering three mutations in 8.3×10^6 bp, given a 'normal' mammalian germ line mutation frequency of 1×10^{-8} per bp per generation (27), is extremely small ($P = 0.0017$; Fisher's exact test). Because ENU was used to generate the *msh6*$^{-/-}$ rat, it could be argued that these mutations are due to the effect of this mutagen in the founder animal. However, analysis of the DNA of the parents showed that all mutations are unique to the progeny and can thus be classified as *de novo* mutations. Furthermore, the lack of any observed spontaneous mutations in 6.6×10^6 bp in wild-type littermates suggests the lack of any experimental biases. In mice, small intestinal epithelial cells from MSH6-deficient animals were shown to exhibit a 41-fold increase in *lac*I mutation frequency compared with wild-type cells (35), which is in line with the ~30-fold increase that we found in the rat germ line.

The observed genomic instability illustrates that the *msh6*$^{-/-}$ rat is a functional gene knockout at the molecular level. As expected, the accumulation of both point and out-of-frame mutations in somatic tissue eventually results in a reduced life span of the MSH6-deficient rat. Although this decrease in life span is also observed in mice lacking MSH6, the survival is considerably longer in the *msh6*$^{-/-}$ rat. Two

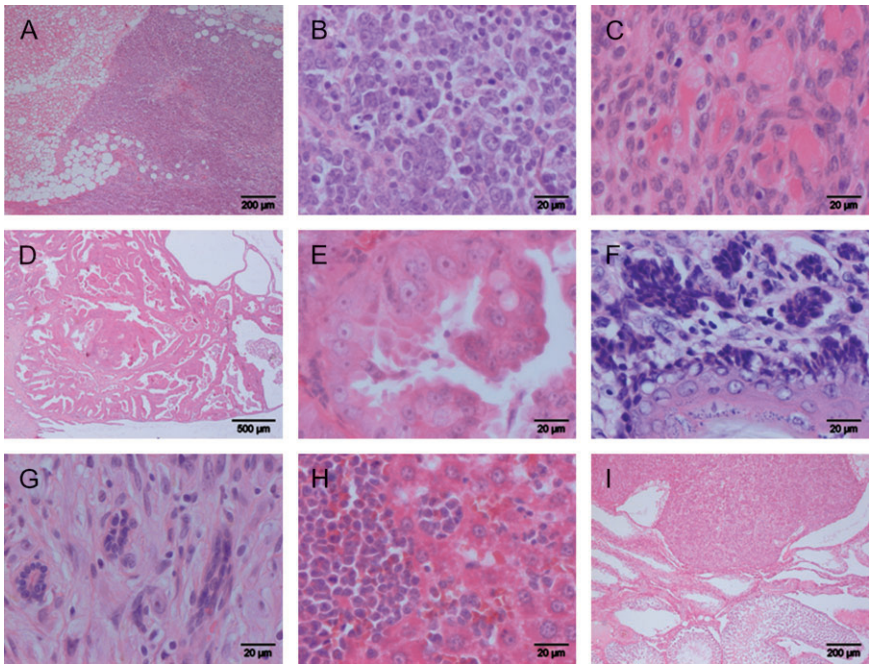

Fig. 3. Tumors observed in the *msh6*$^{-/-}$ rat. (**A**) Section of a mediastinal lymphoblastic lymphoma of an *msh6*$^{-/-}$ male rat stained with hematoxylin and eosin. (**B**) A higher magnification of the lymphoblastic lymphoma. (**C**) Section of a leiomyosarcoma of the endometrium stained with hematoxylin and eosin. (**D**) Section of an endometrial carcinoma stained with hematoxylin and eosin. (**E**) A higher magnification of the endometrial carcinoma. (**F**) A section of a squamous cell carcinoma in the stomach of an *msh6*$^{-/-}$ female rat stained with hematoxylin and eosin. (**G**) Section of a fibroadenoma of an *msh6*$^{-/-}$ male rat stained with hematoxylin and eosin. (**H**) Section of a liver with lymphoblastic lymphoma stained with hematoxylin and eosin. (**I**) Section of a testicle containing a Leydig cell tumor stained with hematoxylin and eosin.

Table II. Tumor spectrum of the MSH6 knockout rat

Rat ID (genotype)	Gender	Age (months)	Tumor type	Tumor size[a] (cm)	Involvement	MSI	
						Mononucleotide repeat[b]	Dinucleotide repeat[c]
17 (−/−)	M	18	B-cell lymphoblastic lymphoma	∼3	Mediastinum	Yes	Yes
25 (−/−)	M	11	B-cell lymphoblastic lymphoma	N/D	Spleen, liver, kidney, lung	No	No
30 (−/−)	F	12	B-cell lymphoblastic lymphoma	∼3	Mediastinum	Yes	Yes
42 (−/−)	M	17	B-cell lymphoblastic lymphoma	N/D	Bone marrow, mediastinum, liver	Yes	Yes
47 (−/−)	F	15	Squamous cell carcinoma	∼2	Stomach	No	No
49 (−/−)	F	12	Leiomyocarcinoma	∼5	Uterus	No	No
52 (−/−)	M	18	Leydig cell tumor	N/D	Testis	No	No
62 (−/−)	M	9	B-cell lymphoblastic lymphoma	N/D	Spleen, liver	Yes	No
68 (−/−)	F	12	Endometrial carcinoma	∼1.5	Uterus	Yes	No
70 (−/−)	F	12	Endometrial carcinoma	∼1	Uterus	Yes	Yes
72 (−/−)	F	18	B-cell lymphoblastic lymphoma	∼1	Mediastinum	Yes	Yes
74 (−/−)	M	14	Fibroadenoma and adenocarcinoma	∼2	Mammary gland	Yes	No
81 (−/−)	F	18	Endometrial carcinoma	∼0.5	Uterus	No	No
85 (−/−)	M	17	T-cell lymphoblastic lymphoma	∼2	Thymus	Yes	No
89 (−/−)	M	10	B-cell lymphoblastic lymphoma	N/D	Spleen, liver	Yes	No

M, male; N/D, not done; F, female.
[a]Approximate tumor diameter estimated from slides.
[b]Two mononucleotide repeats were tested: $(A)_{30}$ and $(G)_{20}$.
[c]Two dinucleotide repeats were tested: $(CA)_{36}$ and $(CA)_{40}$.

different MSH6-deficient mice strains have been generated, both of which have targeted exon 4 of the gene (comparable with the premature stop codon in this report), but on different genetic backgrounds [Msh6^{tm1Rak} was generated in hybrids of C57Bl/6 and WW6 (15); Msh6^{tm1Htr} was generated in hybrids of 129/OLA and FVB (14)]. These models were found to display clear phenotypic differences. For example, the median survival of Msh6^{tm1Rak} mice was found to be 10 months (15), whereas that of Msh6^{tm1Htr} mice was only 6 months (14). The reason why the *msh6*$^{-/-}$ rat shows a delayed onset of tumorigenesis (median survival of 14 months) when compared with the *msh6*$^{-/-}$ mouse models remains unclear. The median life span of wild-type mice and rats do not differ significantly, suggesting that other species-specific characteristics could underlie the observed differences. As rats and mice have diverged for ∼40 million years this is not unlikely. Alternatively, because of its size, the rat could be able to sustain the growth of malignancies longer, allowing tumors to reach relatively larger sizes before the animal becomes moribund. Both the prolonged viability as well as

the capacity of large tumor sizes could allow for longitudinal surgical, chemopreventive and/or therapeutic studies of genetic instable tumorigenesis. Increased life span when compared with similar mouse models was also observed in the *Apc*-mutant Pirc rat, where tumors could reach a diameter >1 cm (22).

The predominant development of lymphomas in the MSH6-deficient rats is also observed in mouse strains lacking MSH6 or other MMR components (13–15,37). The occurrence of human patients with biallelic MMR mutations is rare (38,39), but the cases that have been reported also frequently develop lymphomas, with a relatively early age of diagnosis. A reason for the specificity of lymphoma development can be a high proliferation and turnover rate of lymphocytes during early development. MMR genes *Mhl1*, *Msh2* and *Msh6* play a role in class switch recombination (40–43) and together with a possible increased accumulation of point and out-of-frame mutations, this could rapidly lead to genetic instability and the development of malignant cells. The extensive involvement of the small intestine in the neoplastic phenotype of the Msh6^{tm1Rak} mice (15) was not observed in the rat and could potentially explain the shorter life span of MSH6-deficient mice. However, the Msh6^{tm1Htr} strain rarely develops intestinal tumors, but does show the highest reduction in life span (14). Interestingly, the *msh6*$^{-/-}$ rat shows a high incidence of endometrial cancers (three of seven *msh6*$^{-/-}$ females), resembling the atypical HNPCC spectrum of tumors. Although cancer in the uterus in mice has been reported in the Msh6^{tm1Htr} strain (3 in 22 *msh6*$^{-/-}$ mice), the other MSH6-deficient strain completely lacked involvement of the uterus in their cancer phenotype (14,15), indicating a considerably higher occurrence in the rat. It has been reported that in human families bearing an *Msh6* germ line mutation, the two primary cancers found are colorectal and endometrial cancers (9,44,45). Furthermore, defects in MSH6 have been found to be relatively common in an unselected series of endometrial cancers (46).

There are two major differences between the rat and human cancer phenotypes. First, human HNPCC patient are typically heterozygous for MMR germ line mutations and loose the wild-type allele in somatic cells only. Heterozygous MMR-mutant mice do not develop early-onset tumors, which may be explained by their shorter life span and smaller size (36,47). As for mice, heterozygous MSH6 knockout rats do not develop tumors either (data not shown). However, it should be mentioned that tumors in both human patients as well as the rodent models are MMR deficient. Second, the *msh6*$^{-/-}$ rats do not develop colorectal tumors, but they do show a high incidence of endometrial tumors. It has been suggested that endometrial cancer represents the most common manifestation of HNPCC among female *Msh6* mutation carriers and that colorectal cancer cannot be considered an obligatory prerequisite to define the syndrome (9).

Taken together, the MSH6 knockout rat described here complements existing models for studying DNA MMR and its relation to human genetic instable tumorigenesis. Not only the extended range of phenotypic characteristics but also the size of the animal, the prolonged viability and the ability to bear large sized tumors make this rat an attractable model for specific experimental manipulations, such as endoscopy and local irradiation experiments for studying and treating residual tumor cells.

Supplementary material

Supplementary Figure 1, Tables I and II can be found at http://carcin.oxfordjournals.org/

Funding

'Exploiting natural and induced genetic variation in the laboratory rat' award from the European Heads of Research Councils to E.C.; European Young Investigator, European Science Foundation; Cancer Genomics Centre (Nationaal Regie Orgaan Genomics).

Acknowledgements

The authors thank I.J.Nijman for bioinformatic help, J.van der Belt for technical assistance and H.Feitsma for critically reading the manuscript.

Conflict of Interest Statement: None declared.

References

1. Lahue,R.S. *et al*. (1989) DNA mismatch correction in a defined system. *Science*, **245**, 160–164.
2. Jiricny,J. (2006) The multifaceted mismatch-repair system. *Nat. Rev. Mol. Cell Biol.*, **7**, 335–346.
3. Claij,N. *et al*. (2002) Methylation tolerance in mismatch repair proficient cells with low MSH2 protein level. *Oncogene*, **21**, 2873–2879.
4. Claij,N. *et al*. (2003) DNA mismatch repair deficiency stimulates *N*-ethyl-*N*-nitrosourea-induced mutagenesis and lymphomagenesis. *Cancer Res.*, **63**, 2062–2066.
5. Yang,G. *et al*. (2004) Dominant effects of an Msh6 missense mutation on DNA repair and cancer susceptibility. *Cancer Cell*, **6**, 139–150.
6. Karran,P. *et al*. (1992) Self-destruction and tolerance in resistance of mammalian cells to alkylation damage. *Nucleic Acids Res.*, **20**, 2933–2940.
7. Fishel,R. (1999) Signaling mismatch repair in cancer. *Nat. Med.*, **5**, 1239–1241.
8. Lynch,H.T. *et al*. (1996) Hereditary nonpolyposis colorectal cancer (Lynch syndrome). An updated review. *Cancer*, **78**, 1149–1167.
9. Wijnen,J. *et al*. (1999) Familial endometrial cancer in female carriers of MSH6 germline mutations. *Nat. Genet.*, **23**, 142–144.
10. Ionov,Y. *et al*. (1993) Ubiquitous somatic mutations in simple repeated sequences reveal a new mechanism for colonic carcinogenesis. *Nature*, **363**, 558–561.
11. Boland,C.R. *et al*. (1998) A National Cancer Institute Workshop on Microsatellite Instability for cancer detection and familial predisposition: development of international criteria for the determination of microsatellite instability in colorectal cancer. *Cancer Res.*, **58**, 5248–5257.
12. Reitmair,A.H. *et al*. (1996) Spontaneous intestinal carcinomas and skin neoplasms in Msh2-deficient mice. *Cancer Res.*, **56**, 3842–3849.
13. de Wind,N. *et al*. (1995) Inactivation of the mouse Msh2 gene results in mismatch repair deficiency, methylation tolerance, hyperrecombination, and predisposition to cancer. *Cell*, **82**, 321–330.
14. de Wind,N. *et al*. (1999) HNPCC-like cancer predisposition in mice through simultaneous loss of Msh3 and Msh6 mismatch-repair protein functions. *Nat. Genet.*, **23**, 359–362.
15. Edelmann,W. *et al*. (1997) Mutation in the mismatch repair gene Msh6 causes cancer susceptibility. *Cell*, **91**, 467–477.
16. Lazar,J. *et al*. (2005) Impact of genomics on research in the rat. *Genome Res.*, **15**, 1717–1728.
17. Smits,B.M. *et al*. (2006) Rat genetics: the next episode. *Trends Genet.*, **22**, 232–240.
18. Gibbs,R.A. *et al*. (2004) Genome sequence of the Brown Norway rat yields insights into mammalian evolution. *Nature*, **428**, 493–521.
19. Smits,B.M. *et al*. (2006) Generation of gene knockouts and mutant models in the laboratory rat by ENU-driven target-selected mutagenesis. *Pharmacogenet. Genomics*, **16**, 159–169.
20. Zan,Y. *et al*. (2003) Production of knockout rats using ENU mutagenesis and a yeast-based screening assay. *Nat. Biotechnol.*, **21**, 645–651.
21. Moser,A.R. *et al*. (1990) A dominant mutation that predisposes to multiple intestinal neoplasia in the mouse. *Science*, **247**, 322–324.
22. Amos-Landgraf,J.M. *et al*. (2007) A target-selected Apc-mutant rat kindred enhances the modeling of familial human colon cancer. *Proc. Natl Acad. Sci. USA*, **104**, 4036–4041.
23. Rowley,P.T. (2005) Inherited susceptibility to colorectal cancer. *Annu. Rev. Med.*, **56**, 539–554.
24. Hutchinson,J.N. *et al*. (2000) Transgenic mouse models of human breast cancer. *Oncogene*, **19**, 6130–6137.
25. Cotroneo,M.S. *et al*. (2007) Characterizing a rat Brca2 knockout model. *Oncogene*, **26**, 1626–1635.
26. Nickerson,D.A. *et al*. (1997) PolyPhred: automating the detection and genotyping of single nucleotide substitutions using fluorescence-based resequencing. *Nucleic Acids Res.*, **25**, 2745–2751.
27. Drake,J.W. *et al*. (1998) Rates of spontaneous mutation. *Genetics*, **148**, 1667–1686.
28. Warren,J.J. *et al*. (2006) The structural basis for the mutagenicity of O(6)-methyl-guanine lesions. *Proc. Natl Acad. Sci. USA*, **103**, 19701–19706.

29. Kunkel,T.A. *et al*. (2000) DNA replication fidelity. *Annu. Rev. Biochem.*, **69**, 497–529.
30. Loeb,L.A. *et al*. (2003) Multiple mutations and cancer. *Proc. Natl Acad. Sci. USA*, **100**, 776–781.
31. Tomlinson,I. *et al*. (1999) Selection, the mutation rate and cancer: ensuring that the tail does not wag the dog. *Nat. Med.*, **5**, 11–12.
32. Greenman,C. *et al*. (2007) Patterns of somatic mutation in human cancer genomes. *Nature*, **446**, 153–158.
33. Eshleman,J.R. *et al*. (1995) Increased mutation rate at the hprt locus accompanies microsatellite instability in colon cancer. *Oncogene*, **10**, 33–37.
34. Yamamoto,H. *et al*. (1998) Somatic frameshift mutations in DNA mismatch repair and proapoptosis genes in hereditary nonpolyposis colorectal cancer. *Cancer Res.*, **58**, 997–1003.
35. Mark,S.C. *et al*. (2002) Elevated mutant frequencies and predominance of G:C to A:T transition mutations in Msh6(-/-) small intestinal epithelium. *Oncogene*, **21**, 7126–7130.
36. Wei,K. *et al*. (2002) Mouse models for human DNA mismatch-repair gene defects. *Trends Mol. Med.*, **8**, 346–353.
37. Reitmair,A.H. *et al*. (1995) MSH2 deficient mice are viable and susceptible to lymphoid tumours. *Nat. Genet.*, **11**, 64–70.
38. Bandipalliam,P. (2005) Syndrome of early onset colon cancers, hematologic malignancies & features of neurofibromatosis in HNPCC families with homozygous mismatch repair gene mutations. *Fam. Cancer*, **4**, 323–333.
39. Whiteside,D. *et al*. (2002) A homozygous germ-line mutation in the human MSH2 gene predisposes to hematological malignancy and multiple cafe-au-lait spots. *Cancer Res.*, **62**, 359–362.
40. Ehrenstein,M.R. *et al*. (1999) Deficiency in Msh2 affects the efficiency and local sequence specificity of immunoglobulin class-switch recombination: parallels with somatic hypermutation. *EMBO J.*, **18**, 3484–3490.
41. Martomo,S.A. *et al*. (2004) A role for Msh6 but not Msh3 in somatic hypermutation and class switch recombination. *J. Exp. Med.*, **200**, 61–68.
42. Schrader,C.E. *et al*. (1999) Reduced isotype switching in splenic B cells from mice deficient in mismatch repair enzymes. *J. Exp. Med.*, **190**, 323–330.
43. Schrader,C.E. *et al*. (2002) Role for mismatch repair proteins Msh2, Mlh1, and Pms2 in immunoglobulin class switching shown by sequence analysis of recombination junctions. *J. Exp. Med.*, **195**, 367–373.
44. Charames,G.S. *et al*. (2000) Do MSH6 mutations contribute to double primary cancers of the colorectum and endometrium? *Hum. Genet.*, **107**, 623–629.
45. Wagner,A. *et al*. (2001) Atypical HNPCC owing to MSH6 germline mutations: analysis of a large Dutch pedigree. *J. Med. Genet.*, **38**, 318–322.
46. Goodfellow,P.J. *et al*. (2003) Prevalence of defective DNA mismatch repair and MSH6 mutation in an unselected series of endometrial cancers. *Proc. Natl Acad. Sci. USA*, **100**, 5908–5913.
47. Edelmann,L. *et al*. (2004) Loss of DNA mismatch repair function and cancer predisposition in the mouse: animal models for human hereditary nonpolyposis colorectal cancer. *Am. J. Med. Genet. C Semin. Med. Genet.*, **129**, 91–99.

Received January 3, 2008; revised March 17, 2008; accepted April 5, 2008